Journal of Sea Research 91 (2014) 58–69

Contents lists available at ScienceDirect

Journal of Sea Research

journal homepage: www.elsevier.com/locate/seares

Dissolved organic matter dynamics in the oligo/meso-haline zone of wetland-influenced coastal rivers

Nagamitsu Maie [a,*], Satoshi Sekiguchi [a], Akira Watanabe [b], Kiyoshi Tsutsuki [c], Youhei Yamashita [d], Lulie Melling [e], Kaelin M. Cawley [f,1], Eikichi Shima [a], Rudolf Jaffé [f]

[a] School of Veterinary Medicine, Kitasato University, Towada, Aomori 034-8628, Japan
[b] Graduate School of Bioagricultural Sciences, Nagoya University, Furo-cho, Chikusa-ku, Nagoya 464-8601, Japan
[c] Obihiro University of Agriculture & Veterinary Medicine, 2-11 Inadacho-Nishi, Obihiro, Hokkaido 080-8555, Japan
[d] Faculty of Environmental Earth Science, Hokkaido University, North 10, West 5, Kita-ku, Sapporo 060-0810, Japan
[f] Southeast Environmental Research Center, and Department of Chemistry and Biochemistry, Florida International University, 3000 NE 151 Street, North Miami 33181, USA
[e] Sarawak State Tropical Peat Research Laboratory, Jalan Badruddin, 93000 Kuching, Sarawak, Malaysia

ARTICLE INFO

Article history:
Received 18 April 2013
Received in revised form 27 February 2014
Accepted 28 February 2014
Available online 7 March 2014

Keywords:
Dissolved Organic Matter
Dynamics
Excitation–Emission Matrix
River Mixing Zone
Salinity Gradient

ABSTRACT

Wetlands are key components in the global carbon cycle and export significant amounts of terrestrial carbon to the coastal oceans in the form of dissolved organic carbon (DOC). Conservative behavior along the salinity gradient of DOC and chromophoric dissolved organic matter (CDOM) has often been observed in estuaries from their freshwater end-member (salinity = 0) to the ocean (salinity = 35). While the oligo/meso-haline (salinity < 10) tidal zone of upper estuaries has been suggested to be more complex and locally influenced by geomorphological and hydrological features, the environmental dynamics of dissolved organic matter (DOM) and the environmental drivers controlling its source, transport, and fate have scarcely been evaluated. Here, we investigated the distribution patterns of DOC and CDOM optical properties determined by UV absorbance at 254 nm (A_{254}) and excitation–emission matrix (EEM) fluorescence coupled with parallel factor analysis (PARAFAC) along the lower salinity range (salinity < 10) of the oligo/meso-haline zone for three distinct wetland-influenced rivers; namely the Bekanbeushi River, a cool-temperate river with estuarine lake in Hokkaido, Japan, the Harney River, a subtropical river with tidally-submerged mangrove fringe in Florida, USA, and the Judan River, a small, acidic, tropical rainforest river in Borneo, Malaysia. For the first two rivers, a clear decoupling between DOC and A_{254} was observed, while these parameters showed similar conservative behavior for the third. Three distinct EEM-PARAFAC models established for each of the rivers provided similar spectroscopic characteristics except for some unique fluorescence features observed for the Judan River. The distribution patterns of PARAFAC components suggested that the inputs from plankton and/or submerged aquatic vegetation can be important in the Bekanbeushi River. Further, DOM photo-products formed in the estuarine lake were also found to be transported upstream. In the Harney River, whereas upriver-derived terrestrial humic-like components were mostly distributed conservatively, some of these components were also derived from mangrove inputs in the oligo/meso-haline zone. Interestingly, fluorescence intensities of some terrestrial humic-like components increased with salinity for the Judan River possibly due to changes in the dissociation state of acidic functional groups and/or increase in the fluorescence quantum yield along the salinity gradient. The protein-like and microbial humic-like components were distributed differently between three wetland rivers, implying that interplay between loss to microbial degradation and inputs from diverse sources are different for the three wetland-influenced rivers. The results presented here indicate that upper estuarine oligo/meso-haline regions of coastal wetland rivers are highly dynamic with regard to the biogeochemical behavior of DOM.

1. Introduction

Wetlands are distributed over a wide range of biomes, from the tundra to the tropics, and are key components in the global biogeochemical cycles. For example, 15% of global terrestrial carbon flux from rivers to coastal environments is estimated to be derived from wetlands (Hedges et al., 1997), although wetlands cover only 5-8% of the earth's land surface (Mitsch and Gosselink, 2007). While a significant amount of dissolved

* Corresponding author at: 23-35-1 Higashi, Towada, Aomori 034-8628, Japan. Tel.: +81 176 24 9374; fax: +81 176 23 8703.
E-mail address: maie@vmas.kitasato-u.ac.jp (N. Maie).
[1] Current address: Department of Civil, Environmental, and Architectural Engineering and Institute for Arctic and Alpine Research, University of Colorado at Boulder, 1560 30th Street, Boulder, CO 80303, USA.

http://dx.doi.org/10.1016/j.seares.2014.02.016
1385-1101/

organic carbon (DOC) is exported from rivers draining freshwater wetlands (e.g. Moore et al., 2011), tidal pumping and conservative export through tidal creeks and rivers is also found to be the important mechanism of carbon export from coastal wetlands (Tzortziou et al., 2008). The contribution of DOC from mangrove marshes, which cover a large area of the coastal margin of subtropical and tropical regions, may export DOC equivalent to 10% of the total global DOC export from rivers to ocean (Dittmar et al., 2006). Therefore, it is important to unveil the dynamics of DOM in wetland-influenced coastal rivers.

The behavior of riverine DOM during mixing with oceanic water in estuaries has been mainly studied in the context of changes in DOC concentration along salinity gradients (Cauwet, 2002). These studies often assume that rivers mimic channels that transport upstream DOM to the downstream ocean environment. Many studies report that (1) DOM behaves conservatively, (2) a portion of DOM is removed by aggregation and precipitation (non-conservative mixing), and (3) some DOM undergoes losses through microbial degradation during estuarine mixing (non-conservative mixing; references in Cauwet, 2002). Considering these scenarios, Cifuentes and Eldridge (1998) systematically explained the difference in the behavior of riverine DOM in the mixing zone based on the concentration of biodegradable DOM in rivers and the DOC residence time in estuaries.

However, the dynamics of DOM in wetland-influenced coastal rivers is more complex than the simple mixing of upriver-derived DOM with saline water, since additional DOM can be supplied from tidally flooded coastal wetlands, riparian soil/plant residues, exudation from phytoplankton from the flood plains, emergent macrophytes, seagrass, microbial mats, and groundwater inputs (Bertilsson and Jones, 2003; Dittmar et al., 2012; Hedges, 1992; Maie et al., 2006; Tzortziou et al., 2008). Furthermore, in addition to multiple sources of DOC, recent studies have shown changes in the quantity and quality of DOM during mixing with saline water, in which photodegradation was emphasized as an important driver (Cawley et al., 2013; Dalzell et al., 2009; Dittmar et al., 2006; Fellman et al., 2010a). Therefore, DOM dynamics represent a complex balance between source material, degradation processes, and export in coastal wetlands. Considering the diverse hydrological conditions, ecological functions, and biogeochemical characteristics of coastal wetlands, it is difficult to predict DOM dynamics in such ecosystems. In addition, the oligo/meso-haline zone of coastal rivers has been reported to be particularly sensitive to DOC dynamics and frequently reported as being non-conservative with regard to mixing with marine waters (Cauwet, 2002). However, information on comparative studies of this dynamic zone in estuaries with regard to DOM sources and mixing is limited. Adding to the existing knowledge on this subject is the main objective of this study.

The quality (composition) of DOM reflects its origin and diagenetic history, and thus, characterizing physico-chemical properties of DOM provides useful clues in unveiling its biogeochemistry. In order to compare the DOM dynamics across different wetland ecosystems on an equal footing, it is crucial to use identical analytical methods that measure the quality as well as the quantity of DOM. In this respect, fluorescence spectroscopy has been widely applied in DOM characterizations, as it offers high sensitivity and high sample throughput (Coble, 2007; Fellman et al., 2010b; Jaffé et al., 2008). In addition, it requires minimal pretreatment/preparation of the samples, which enables analysis of water samples under nearly natural environmental conditions. One of the most powerful techniques among fluorescence analyses is the combination of excitation–emission fluorescence matrices (EEM) and parallel factor analysis (PARAFAC) (e.g., Cory and McKnight, 2005; Stedmon and Markager, 2005; Yamashita et al., 2008). EEM-PARAFAC can statistically decompose a dataset of EEMs into defined fluorescence contributions such as protein-like and humic-like components, and therefore enables comparative quantitative evaluations for each fluorescent component along environmental gradients or different environmental settings. In particular, EEM-PARAFAC successfully detects small changes in the composition of humic-like fluorophores that are the dominant components of DOM in wetlands (e.g. Cawley et al., 2012a; Chen et al., 2013; Yamashita et al., 2010). Thus, EEM-PARAFAC is considered to be suitable for evaluating similarities and differences of DOM dynamics across wetland/estuarine ecosystems with different environmental characteristics.

The aim of this research was to contribute to the present state of knowledge on DOM dynamics in the oligo/meso-haline zone (salinity < approx. 10) through a comparative study of three wetland-influenced rivers by assessing differences and commonalities in vastly different environmental settings. For that purpose, we conducted high frequency sampling of surface river water along salinity gradients and DOM was characterized using DOC determinations, UV–visible absorption spectroscopy and EEM-PARAFAC. Factors affecting the quantity and the quality of DOM in aquatic environments are very complex, and may include climate (precipitation and thus seasonality), watershed characteristics (e.g. % wetland cover), soil carbon content, and watershed hydrology (Mulholland, 2003). DOM dynamics have been shown to be affected by seasonal variations due to the changes in primary productivity, hydrology, residence time and photo-exposure in wetlands and estuaries (e.g. Asmala et al., 2012; Cawley et al., 2013; Chen et al., 2013; Maie et al., 2012). However, determining in detail the environmental drivers controlling the differences in the quantity and the quality of DOM between the three wetland-influenced rivers, or assessing potential seasonal influences, is beyond the scope of this study. Here we compare the distribution patterns of DOC abundance and optical properties, to elucidate similarities and differences in environmental factors controlling the dynamics of DOM in the oligo/meso-haline zone of three different case studies.

2. Site description

Study sites used in this work were selected to maximize differences in environmental setting, such as climatic region, geomorphology and vegetation cover, but keeping within the commonality of wetland-influenced, estuarine river systems. In addition, site accessibility, logistical support, and previous research on these sites (Watanabe et al., 2012) were important considerations in the selection process.

2.1. Bekanbeushi River, Hokkaido, Japan

The Bekanbeushi River is located in the eastern part of Hokkaido, the northernmost of Japan's four major islands (Fig. 1a). The area has a cool-temperate climate (Dfb) where the average annual temperature and precipitation are 6.6 °C and 1448 mm, respectively (Japan Metrological Agency 2010). The river flows through a low moor, namely Bekanbeushi Moor, where reed, carex, and *Alnus japonica* grow, and empties into Lake Akkeshi. The total length of the river is 43 km and its watershed area is 555.7 km^2, of which 53.1, 24.7, and 15.3% are covered with forests, agricultural lands, and wetlands, respectively (Woli et al., 2004). Lake Akkeshi is an enclosed brackish lake with an area of 32.3 km^2 and an average depth of 2 m. The bottom of the lake is largely covered by seagrasses such as *Zostera marina* and *Zostera japonica*. Lake Akkeshi is connected to the Akkeshi Bay by a narrow channel, 600 m in width and an average 10 m in depth. Tidal effects from the bay are known to influence to lower reaches of the Bekanbeushi River.

2.2. Harney River, South Florida, USA

The Everglades, located in the southern tip of the Florida Peninsula, USA, is among the largest subtropical wetlands in the world (Fig. 1b). The average annual temperature is 25 °C and the average precipitation is 1521 mm. The Everglades are characterized by well-defined wet (May–October) and dry (November–April) seasons, which have shown to influence DOM dynamics in the system (Chen et al., 2013). Waters from Everglades National Park flow through a shallow inland freshwater marsh dominated by emergent wetland plants such as

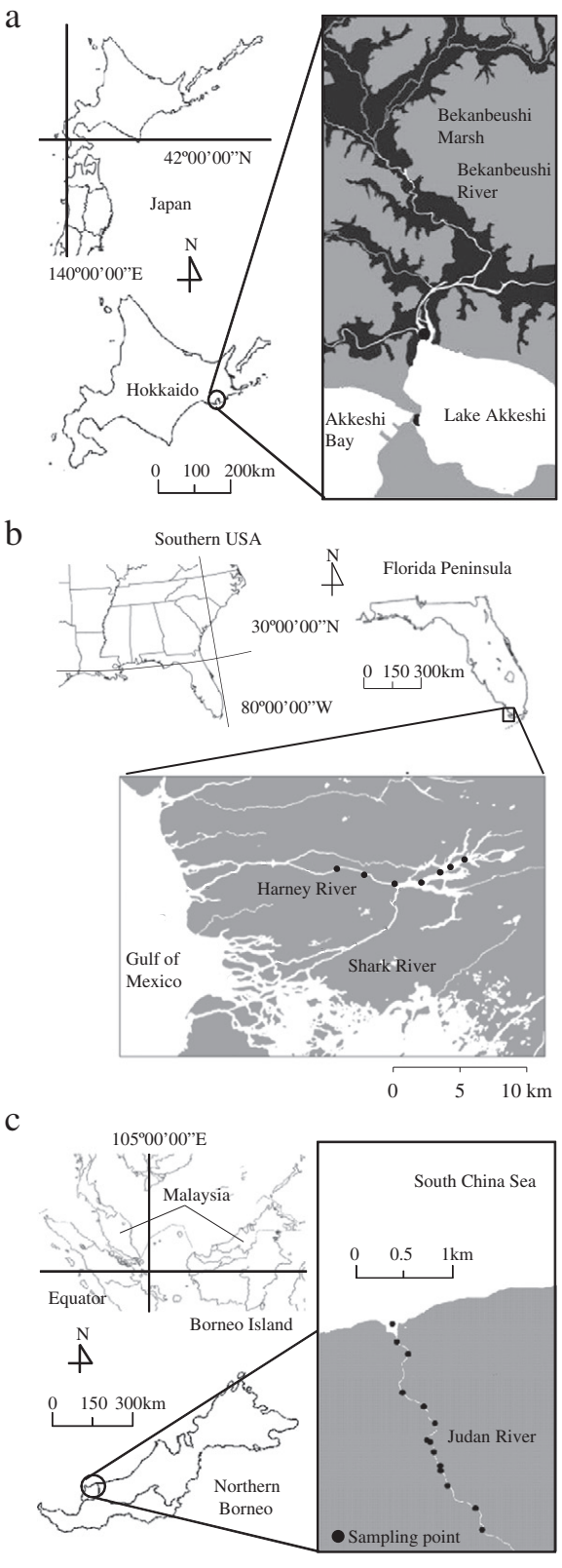

Fig. 1. Map of sampling sites.

Cladium and *Eleocharis*, and an abundance of calcareous periphyton mats. The vegetation of the watershed shifts to tidally submerged mangrove marshes at the lower reaches, where tidal mangrove rivers such as the Harney River connect the freshwater wetlands with the Gulf of Mexico. More detail on the watershed characteristics of the Everglades can be found elsewhere (Davis and Ogden, 1994).

2.3. Judan River, Sarawak, Malaysia

Sarawak is located in the northwestern part of Borneo Island, has a tropical rainforest climate (Af; Fig. 1c). Monthly average maximum and minimum temperature ranges from 29 to 33 °C and 22 to 23 °C, respectively. Average annual precipitation is 3904 mm. Sarawak has a broad wet season accompanied by monsoons from November to February. The Judan River flows through the southwest part of Sarawak (N2°53′41″ E111°59′94″) and directly enters into the South China Sea where the coastal line is fringed with sandy beaches. The total length of the river is 23 km, and local people who live along the river use it for transportation. Along the river, mixed riparian swamp forests have developed on peat soil. Dominant vegetation is characterized by tropical trees, namely Ramin (*Gonystylus bancanus*), Jongkong (*Dactylocladus stenostachys*), Kapur (*Dryobalanops rappa*), and Alan (*Shorea albida*).

3. Materials and methods

3.1. Sample collection and sample preparation

A suite of fluvial water samples were collected at different salinities using a canoe/boat at the Bekanbeushi River and Lake Akkeshi during base flow (30 samples; August 2009, summer), at the Harney River (7 samples; March 2010, dry season), and at the Judan River (15 samples; August 2009, dry season). In all cases, surface waters were collected for DOM characterization only at the low salinity range of the low/meso-haline zone (salinity < approx. 10). Water samples were collected in prewashed 100-mL amber polypropylene sample bottles (Nalgen®, Nalge Nunc Inc; presoaked in 0.5 M HCl followed by 0.1 M NaOH for 4 h each). Water samples were put on ice and brought back to the laboratory in a cooler. They were filtered immediately through a precombusted (450 °C for 4 h) glass fiber filter (GB-140, ADVANTEC, nominal pore size, 0.4 μm or GF/F, Whatman, nominal pore size, 0.7 μm) to remove suspended solids, and the filtered water samples were kept in a refrigerator (4 °C) until analysis (maximum, 1 week). Field measurements of salinity and pH were conducted on site using YSI multiparameter sondes or equivalent.

3.2. Analysis of DOC concentrations and UV-visible spectra

DOC concentrations were determined with a Shimadzu TOC-V_{CPN} analyzer (Kyoto, Japan). Filtered samples were acidified with 1.5% (v/v) 3 M HCl in a built-in syringe of the analyzer and were purged with CO_2-free air for 90 s to remove inorganic carbon prior to analysis. UV–Vis absorbance spectra of filtered water samples derived from the Bekanbeushi and Judan Rivers were measured in a 5-cm quartz cell on a UV–Vis spectrophotometer (UV-1800, Shimadzu) from 240 to 700 nm at 2.0-nm increments. The water samples from Harney River were analyzed using another spectrophotometer (Cary 50 Bio, Varian) according to procedure described in Yamashita et al. (2010). Absorption at 254 nm (A_{254}) reported in this study is often used as a proxy for aromatic carbon concentration in DOM and as a measure of relative concentrations of CDOM or dissolved humic substances in river water (Chin et al., 1994; Weishaar et al., 2003).

3.3. EEM-PARAFAC analysis

Excitation–emission matrix (EEM) fluorescence spectra of the filtered water samples were determined using a spectrofluorometer (FluoroMax-3 or FluoroMax-4, Horiba Jobin Yvon) equipped with a 150-W xenon lamp as the light source. Samples for EEM of the Judan River samples were measured after diluting 5 times with Milli-Q water, since the UV–Vis absorption was too high for proper fluorescence determinations. Using the FluoroMax-4, each EEM of samples derived from the Bekanbeushi and Judan Rivers was determined using an excitation wavelength (λ_{ex}) profile from 240 to 550 nm at increments of 5 nm, and the emission signal was scanned in the range of 290 to 600 nm at increments

of 2 nm (Abe et al., 2011). The band pass was set at 5 nm for both excitation and emission wavelengths. To avoid any influence of possible wavelength dependency and fluctuation of the excitation lamp output, all fluorescence spectra were acquired as a ratio of sample (emission signal; S) and reference (excitation lamp output; R) signals. Water samples from Harney River were analyzed using FluoroMax-3 according to Yamashita et al. (2010). The inner filter effect was corrected according to McKnight et al. (2001), and each EEM sample was corrected for Raman scattering and background fluorescence by subtracting the spectra of a Milli-Q water (Millipore) blank. The intensity of the EEM spectra was normalized using quinine sulfate and expressed as quinine sulfate unit (QSU).

To decompose EEMs into distinct fluorescent components, data were further statistically analyzed using parallel factor analysis (PARAFAC, Stedmon and Bro, 2008; Stedmon et al., 2003) with the DOMFluor toolbox (Stedmon and Bro, 2008) using MATLAB software (ver. 7.7; MathWorks, Inc.). PARAFAC was performed separately for each wetland using datasets which consisted of water samples collected from each of the three studied river systems and adjacent river/wetland ecosystems (including some shallow (<70 cm) groundwater samples for the Judan River area). Thus, we report EEM-PARAFAC results derived from three distinct models in this study (Table 1 and Fig. 3). Specifically, the numbers of EEMs used for PARAFAC analysis were 147 and 501 for the Bekanbeushi and Judan Rivers, respectively. The dataset of the Bekanbeushi River was composed of Bekanbeushi River samples and surface water samples collected from wetland-influenced rivers in the east and southeast part of Hokkaido (Fig. 1). Dataset of the Judan River consisted of Judan River samples and groundwater samples (shallower than 70 cm) of an oil palm plantation reclaimed on tropical peat soil in Naman, Sarawak, located 80 km south of the Judan river mouth. The Harney River EEMs were fit to an existing eight component PARAFAC model described in Chen et al. (2010) and Yamashita et al. (2010) that was comprised of Florida coastal Everglades samples (n = 1394). The spectroscopic region of EEMs used in the analysis employed an excitation wavelength of 260–450 nm and emission wavelength of 300–500 nm for Bekanbeushi River, and an excitation wavelength of 260–500 nm and emission wavelength of 300–550 nm for Judan River, respectively. The validity of the model was confirmed by split-half analysis and Tucker's congruence coefficients (Stedmon and Bro, 2008). Such analysis using three PARAFAC models allows for the comparison of DOM characteristics, in terms of similarities and differences, among three different coastal wetlands. PARAFAC components for the different models were identified as C1 to CX (component numbers ranging from 1 to X), and with a subscript as B, H, and J for the Bekanbeushi, Harney and Judan rivers, respectively.

4. Results

4.1. DOC and A_{254} distributions

The distribution patterns of DOC and A_{254} with increasing salinity for three wetland-influenced rivers are shown in Fig. 2. The DOC ranges were 0.26–0.36, 1.4–1.5, and 3.0–3.7 mmol L^{-1} for the Bekanbeushi River, Harney River, and Judan River, respectively. In the same order, the A_{254} ranges were 13.0–22.8 m^{-1}, 63.2–65.4 m^{-1}, and 185–235 m^{-1}. The pH ranges were 7.2–7.3, 7.7–8.0, and 3.9–6.2 for the Bekanbeushi, Harney, and Judan Rivers, respectively.

The distribution patterns of DOC and A_{254} along the salinity gradient were correlated for the Judan River but decoupled for the Bekanbeushi River and Harney River (Fig. 2). At the Bekanbeushi River, DOC and A_{254} were higher in the lower salinity range (salinity <2.5) than for the estuarine lake water (Salinity = ca. 11). However, DOC did not drop systematically with the increase in salinity while A_{254} decreased conservatively. This result suggests that, although the proportion of colored DOM decreased toward estuarine lake, additional DOC sources at salinities between 0.5 and 1.5 were also observed. It should be noted that A_{254} at Lake Akkeshi (salinity = 11) was close to the extrapolated regression line between A_{254} and salinity that was estimated using the data at salinity range of <2.5. These distributional patterns imply that major fractions of CDOM behave conservatively during the mixing process with the estuarine lake water, but there is a non-colored DOM source along the river-lake interface.

Table 1
Assignment of EEM-PARAFAC components.

Traditional peak assignment	Peak characteristics	Bekanbeushi River		Harney River		Judan River		Cory and McKnight (2005)	Stedmon and Markager (2005)
		Comp. ID	Ex / Em (nm)	Comp. ID	Ex / Em (nm)	Comp. ID	Ex / Em (nm)		
Peak C	Ubiquitous humic-like peak	$C2_B$	<260 (320)[a] / 422	$C6_H$	<260 (325) / 406			SQ3[b]	6 (Ant) <250 (320) / 400
		$C1_B$	<260 (345) / 480	$C1_H$	<260 (345) / 462	$C1_J$ $C6_J$	<260 (330) / 458 305 (260) / 448	C1	4_Ter/Aut <250 (360) / 440
	Terrestrial humic-like, fulvic acid-type	$C3_B$	<260 (310) / 426	$C3_H$	<260 (305) / 416	$C5_J$	295 / 406	C10	3_Ter <250 (305) / 412
	Undefined					$C2_J$	275 (390) / 474	SQ2[b]	
Peak A	Terrestrial humic-like Photo-refractory or photodegradation product (Stedmon et al., 2007)	$C5_B$	<260 / 472	$C2_H$	<260 / 454	$C3_J$	<260 / 466	Q1 or Q2	1_Ter[c] <250 / 448
Peak M	Microbial-humic like · Autochthonous	$C6_B$	300 (<260) / 376	$C4_H$	<260 (305) / 376			C3[b] or Q3[b]	
Undefined	Terrestrial humic-like, humic acid-type	$C4_B$	<260 / >500	$C5_H$	275 (405) / >500	$C4_J$	<260 / >530	SQ1	2_Ter/Aut <250 (385) / 504
Peak B or T	Protein-like materials (Yamashita and Tanoue, 2003)	$C7_B$	275 / 326 (414)	$C7_H$	275 / 326			Trp	(7_Aut) 280 / 344
Peak B	Protein-like materials (Yamashita and Tanoue, 2003)			$C8_H$	300 / 342			Trp	(7_Aut) 280 / 344

[a] Numbers in parentheses refer to the second maximum.
[b] Only present in the Antarctic samples, indicating microbial origin.
[c] Ter, Ant, and, Aut refer to terrestrial, anthropogenic, and autochthonous origins, respectively.

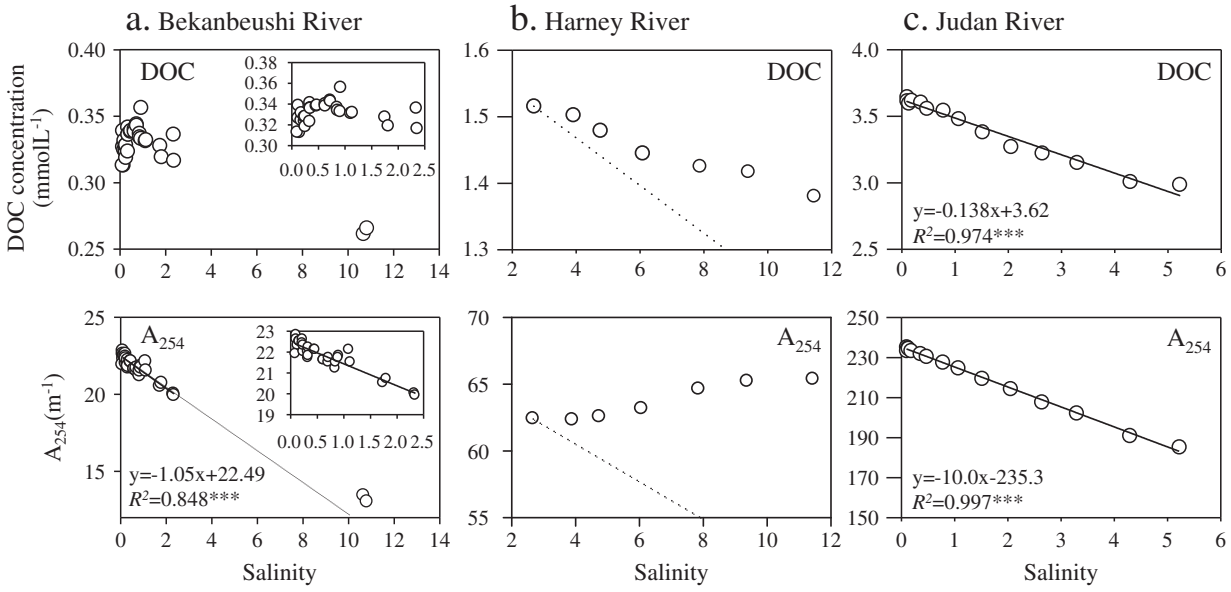

Fig. 2. Changes in DOC and A_{254} along salinity gradients. Line for Bekanbeushi River refers to a regression line, which was calculated excluding the data at the salinity near 11. Dotted line for Harney River is a simple conservative mixing line between terrestrial (salinity 2) and marine end members (salinity 32). Lines for Judan River are regression lines.

For the Harney River, the distribution patterns of DOC and A_{254} along the salinity gradient showed contrasting trends, where the DOC decreased while A_{254} increased with the increase of salinity, suggesting the input of highly colored DOM. Cawley et al. (2013) reported non-conservative behavior of DOC and UV absorbance for the Harney River, especially at low to mid salinity ranges, indicating that mangrove ecosystems export a significant amount of DOM to the river. The contrasting trends between DOC and A_{254} at low salinity range in the mesohaline zone of the Harney River suggest that DOM having a high light absorbing capacity is exported from the mangrove fringe.

At the Judan River, both DOC and A_{254} apparently decreased linearly with the increase of salinity, suggesting that the conservative mixing is the dominant process in the oligohaline zone of this river.

4.2. PARAFAC models

EEMs collected from the Bekanbeushi River were decomposed into 7 PARAFAC components (Table 1 and Fig. 3). The assignments of peaks are listed in Table 1. One component, $C3_B$, and two components, $C1_B$ and $C2_B$, are assigned as terrestrial fulvic acid-type component and ubiquitous humic-like component, respectively. These components can be categorized as traditional terrestrial humic-like peak C (Coble et al., 1998). $C5_B$ is categorized as a terrestrial humic-like component similar to the traditional terrestrial humic-like peak A. $C6_B$ is assigned as a microbial humic-like component (traditional peak M). $C4_B$ could not be categorized by a traditional definition but was assigned as terrestrial humic acid-type component based on its spectral characteristics. One protein-like component, $C7_B$, was also identified in this EEM-PARAFAC model.

EEMs collected from Harney River were decomposed by fitting to an existing 8 component model that was obtained using data collected from the Greater Everglades (n = 1394). Details in the eight components can be found elsewhere (Chen et al., 2010; Maie et al., 2012; Yamashita et al., 2010). Briefly, three components ($C1_H$, $C3_H$, and $C6_H$) were categorized as humic-like components similar to the traditional peak C (Table 1 and Fig. 3), where $C6_H$ has been suggested to have a microbial origin (Yamashita et al., 2010). $C2_H$ and $C4_H$ were assigned as humic- and microbial humic-like components, similar to the traditional peaks A and M, respectively. A humic acid-type (but undefined by traditional definitions) was also evident as $C5_H$. Two components, $C7_H$ and $C8_H$, were categorized for protein-like components.

The PARAFAC analysis of the Judan River decomposed the EEM dataset into 6 PARAFAC components, for which properties and assignments are listed in Table 1 and Fig. 3. Three of those ($C1_J$, $C5_J$, and $C6_J$) were related to the traditional peak C. $C1_J$ and $C6_J$ could be categorized as ubiquitous humic-like components, while $C5_J$ as terrestrial humic-like component. A component with spectral characteristics similar to the traditional peak A was also evident as $C3_J$. In analogy with the Bekanbeushi River and Harney River, one component ($C4_J$) was assigned as an undefined, terrestrial humic-acid type component. A unique component, $C2_J$, was only observed in the Judan River PARAFAC model. Note that protein-like components were not identified in the Judan River PARAFAC model.

4.3. Distributions of PARAFAC components

The distributions of each PARAFAC component vs. salinity for the Bekanbeushi River are shown in Fig. 4. The fluorescence intensities of components, $C1_B$, $C2_B$, and $C3_B$, defined as related to the terrestrial humic-like peak C, tended to decrease as the salinity increased at the low salinity range, and were lowest in the estuarine lake. The greatest correlation with salinity was found for $C1_B$. Similar distribution pattern was also evident for terrestrial humic acid type component $C4_B$. On the other hand, the terrestrial humic-like component $C5_B$, analogous to the terrestrial humic-like peak A, significantly increased with the salinity in the low salinity range and was highest in the estuarine lake. The microbial humic-like component $C6_B$ and protein-like component $C7_B$ did not show any consistent trend with the change of salinity, even though the intensities of $C6_B$ were higher in river waters than in the estuary lake waters. These results suggested that terrestrial humic-like components (except for $C5_B$) mixed conservatively during freshwater–seawater mixing. On the other hand, autochthonous contributions seem important in controlling the levels of microbial humic-like and protein-like components in Bekanbeushi Marsh.

For the Harney River, terrestrial humic-like component $C3_H$, microbial humic-like component $C4_H$, and the two protein-like components $C7_H$ and $C8_H$ showed nearly conservative behavior (Fig. 5). However, terrestrial humic-like components, $C1_H$, $C5_H$, and $C6_H$ showed non-conservative behavior at salinity ranges from ~5 to 11, suggesting their significant inputs from the mangrove fringe.

A unique distribution pattern of PARAFAC components along the salinity gradient was observed for the Judan River (Fig. 6). Significant

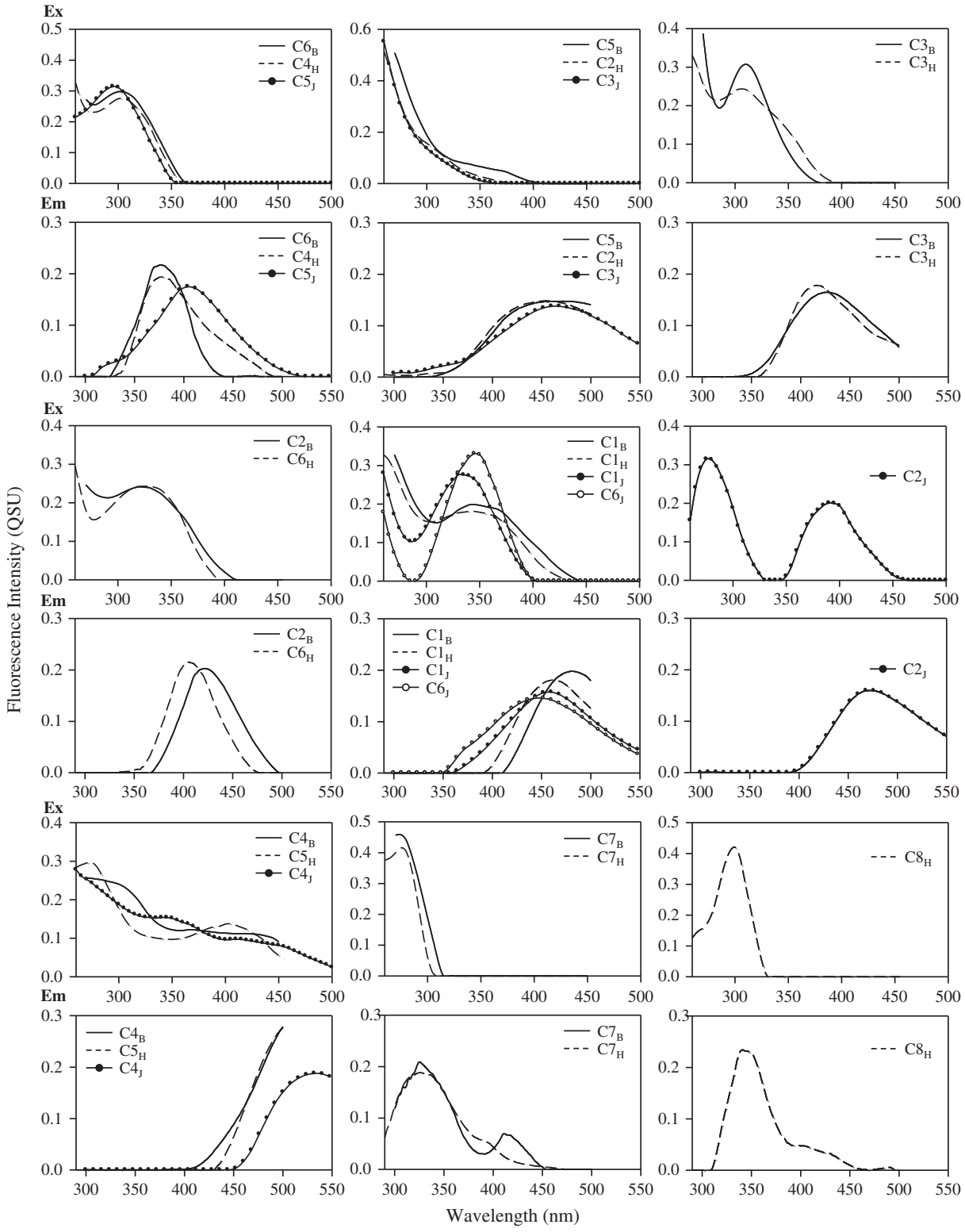

Fig. 3. Excitation–emission characteristics of PARAFAC components. Component (C) with subscript B, H, J, refers to the components found from Bekanbeushi, Harney, and Judan Rivers, respectively.

decreases in the fluorescence intensity were observed for the ubiquitous humic-like component $C1_J$, the terrestrial humic acid-type component $C4_J$, and the terrestrial humic-like component $C5_J$ with increases in salinity. Interestingly, the other two humic-like components, $C2_J$ and $C6_J$, increased significantly while the terrestrial humic-like component $C3_J$ did not show any trend with the increase of salinity.

5. Discussion

5.1. PARAFAC components identified from three coastal wetlands

Three distinct sets of PARAFAC components were obtained from three wetland rivers from different climatic zones, i.e., cool-temperate, subtropical, and tropical regions (Table 1 and Fig. 3), which had

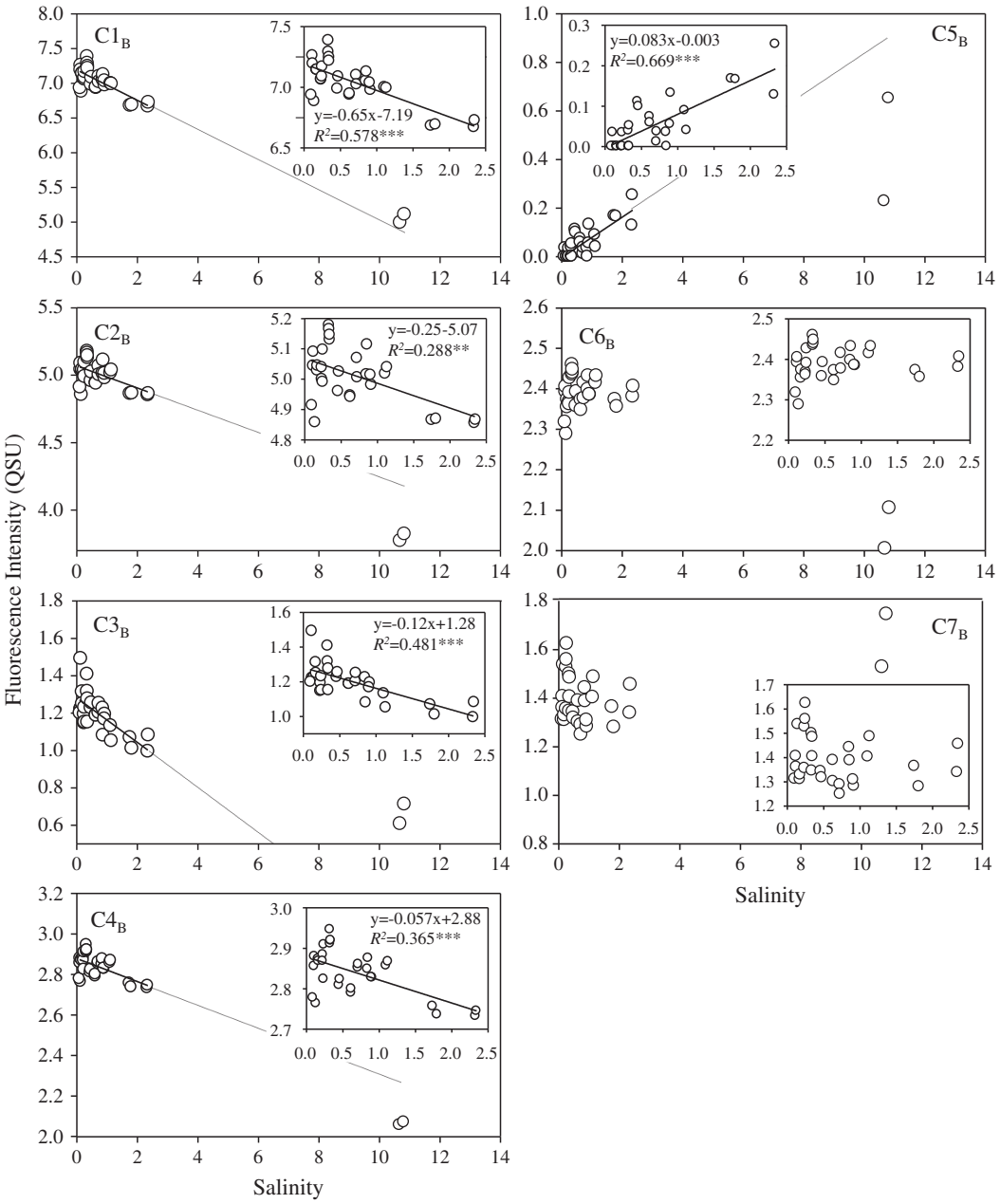

Fig. 4. Changes in the intensities of 7 PARAFAC components along the salinity gradient for the Bekanbeushi River. Lines in plots are regression lines, which were calculated excluding the data at the salinity near 11. Dotted lines are extrapolated portion of the regression line.

previously been shown to have compositional differences in their DOM with regard to their humic and non-humic substance abundance (Watanabe et al., 2012). It is noteworthy that PARAFAC components with similar characteristics were found in the three distinct models, indicating the occurrence of similar fluorophores in the three wetland-influenced rivers. The characteristic components found for three models were related to: (1) the traditional peak C defined by Coble et al. (1998), or ubiquitous, fulvic acid-type fluorescence components defined by other PARAFAC models (Santín et al., 2009; Yamashita et al., 2010), (2) the traditional peak A, or terrestrial humic-like fluorescence component that had been suggested as a photo-refractory or as photo-degradation product (Cawley et al., 2012a; Chen et al., 2010; Maie et al., 2012; Stedmon et al., 2007), (3) a traditionally undefined, humic acid-type fluorescence component (Ohno and Bro, 2006; Santín et al., 2009), (4) the traditional peak M, or microbial humic-like fluorescence component (Coble et al., 1998), and (5) the protein-like components defined as tryptophan or tyrosine-like fluorescence. These PARAFAC components have commonly been reported in a wide range of terrestrial aquatic environments as well as coastal environments (e.g., Cory and McKnight, 2005; Fellman et al., 2009; Fellman et al., 2011; Stedmon and Markager, 2005; Yamashita et al., 2008). According to a review by Ishii and Boyer (2012), humic-like components reported in this study are commonly found in terrestrial and coastal aquatic environments. Therefore, the similarity in the PARAFAC components among the three study sites suggests that the site selection is adequate to perform a comparative DOM dynamics study among the three rivers featuring vast differences in geomorphology, vegetation cover, hydrology, and climate. It is notable that a unique component, $C2_J$, was only detected in the Judan River (Table 1 and Fig. 3). This type of PARAFAC component has occasionally been reported in surface waters and was assigned as humic/fulvic acid-like peak of terrestrial origin (Cory and McKnight, 2005; Lapierre and Frenette, 2009; Osburn and Stedmon, 2011; Singh et al., 2010; Stedmon and Markager, 2005; Williams et al., 2010).

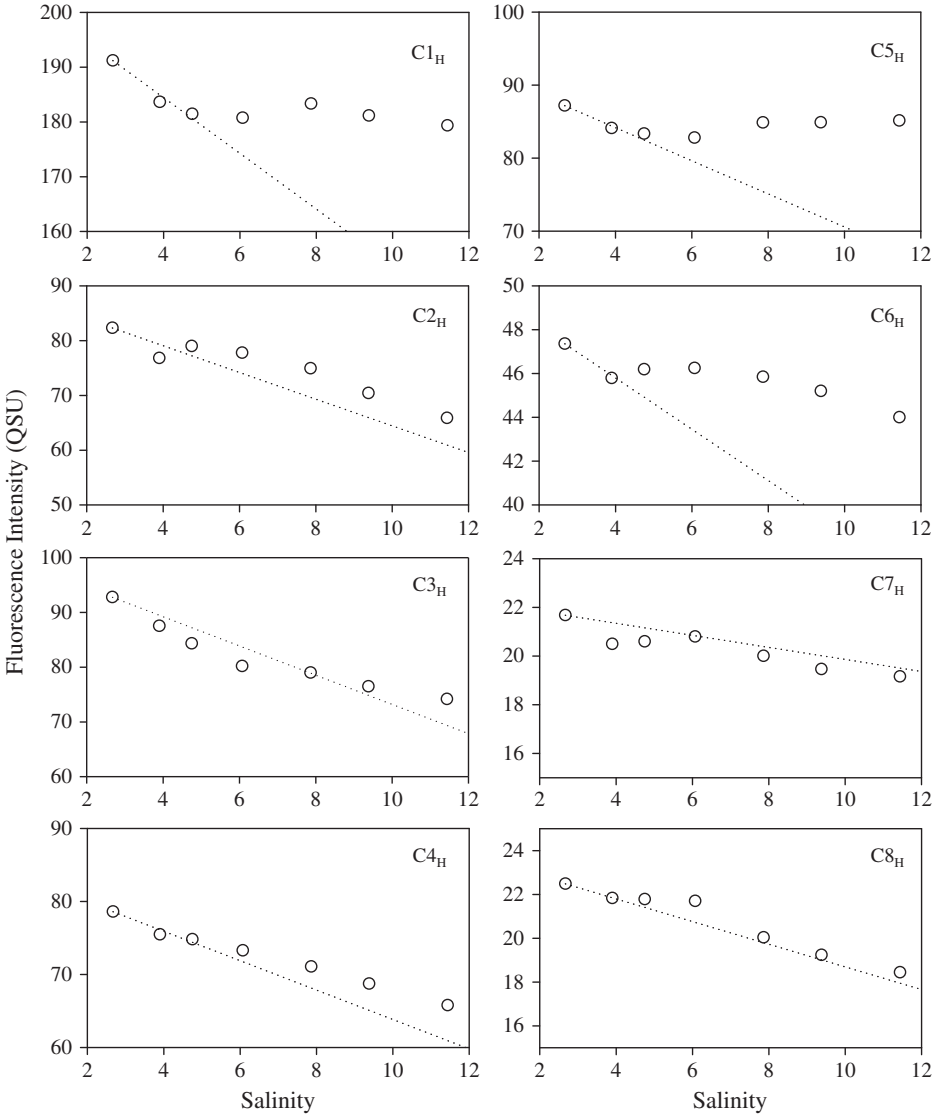

Fig. 5. Changes in the intensities of 8 PARAFAC components along salinity gradients for Harney River. Dotted lines are conservative mixing lines for each components between terrestrial (salinity 2) and marine end members (salinity 34).

5.2. Environmental dynamics of DOM

The distribution patterns of DOC and A_{254} were largely different among the three wetland rivers (Fig. 2). The DOC levels were in the order of Judan River (tropical climate) > Harney River (subtropical climate) > Bekanbeushi River (cool-temperate climate). The SUVA value, which is the UV-absorbance at 254 nm normalized by DOC concentration, and a proxy for the aromaticity of DOM (Weishaar et al., 2003), ranged between 4.95 and 5.93, 3.43 and 3.94, and 5.17 and 5.46 for the Bekanbeushi River, Harney River, and Judan River, respectively, suggesting a lower aromatic nature in the mesohaline zone for the Harney River. This may be the result of DOM enriched in microbial sources (periphyton-derived) entering the upper Harney estuary from the freshwater Everglades marshes (Chen et al., 2013).

Thus, the estimation of DOC concentration from simple linear correlations with CDOM, especially for estuaries with autochthonous DOM contributions in addition to terrestrial end-member inputs, needs to be considered with caution. Recently, Fichot and Benner (2011) successfully estimated the DOC concentration in the Gulf of Mexico using a CDOM spectral slope parameter obtained between 275 and 259 nm, but indicated that local parameterization is necessary for the better estimation of DOC concentration due to differences in DOM sources and regulatory processes among coastal environments. Similarly, in an effort to determine optical proxies for DOC concentration in boreal estuaries, Asmala et al. (2012) reported that the correlation between DOC and CDOM (A_{254}) concentrations was not consistent throughout the year, but varied seasonally with changes in source strength and diagenetic processing (i.e. photobleaching). In agreement with these reports our results also suggest that DOC proxies derived from absorbance or fluorescence values should be tested for individual estuarine environments, particularly for the oligo/meso-haline zone. In addition to DOC and A_{254}, the PARAFAC components behaved differently among three rivers, where noticeable differences were observed in the distribution patterns of humic acid-type components ($C4_B$, $C5_H$, $C4_J$) and peak C type components ($C1_B$, $C2_B$, $C3_B$, $C1_H$, $C3_H$, $C6_H$, $C1_J$, $C5_J$, and $C6_J$). Differences in both quantitative values and qualitative DOM characteristics for the low salinity zones suggest that ample variations in DOM dynamics control the distribution of these biogeochemical parameters for different river environments, and that salinity should not be used as a proxy to assess DOC dynamics in low salinity, upper estuarine areas of wetland-influenced coastal rivers.

In the following section, we discuss the characteristics of the distribution of the fluorescence components and their controlling environmental factor(s) by comparing the three rivers.

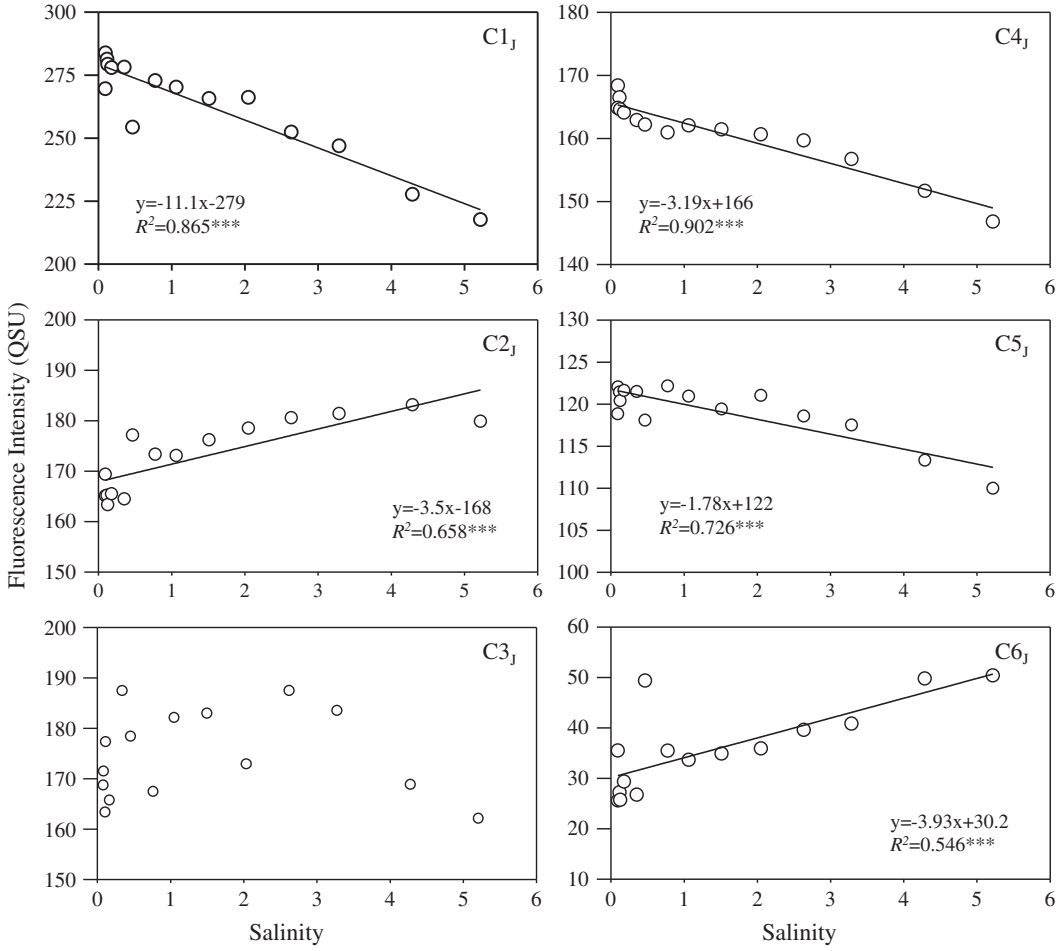

Fig. 6. Changes in the intensities of 6 PARAFAC components along salinity gradient for Judan River. Lines are regression lines.

5.3. Bekanbeushi River case study

In the Bekanbeushi River, the A_{254} decreased while the DOC remained relatively constant along the salinity gradient. In addition, while ubiquitous and terrestrial fulvic acid-type ($C1_B$, $C2_B$, $C3_B$) and humic acid-type ($C4_B$) components were basically distributed conservatively, the protein-like ($C7_B$) and the microbial humic-like ($C6_B$) components behaved non-conservatively. This incongruity can be attributed to a diversity of DOM source, where a major portion of dissolved humic substances are of terrestrial origin, whereas a significant portion of non-colored DOM is of estuarine origin. The bottom of Lake Akkeshi is largely covered by *Z. marina*, *Z. japonica*, and associated epiphytic algae, which are characterized by high primary productivity (Hasegawa et al., 2007). Seagrass/epiphytic algae communities exudate a significant portion of DOM produced during photosynthesis (Barrón et al., 2012; Bertilsson and Jones, 2003; Ziegler and Benner, 1999), which may contribute to the high level of autochthonous non-colored DOM in the estuarine lake (Cawley et al., 2012b; Maie et al., 2005).

$C6_B$ and $C7_B$ kept a similar level at the low salinity range, while their intensities shifted lower and higher, respectively, in Lake Akkeshi. This result suggests high microbial activity in the mixing zone, since otherwise $C6_B$ and $C7_B$ would show conservative mixing similar to some components of the Harney River ($C4_H$ and $C7_H$). The relatively constant abundance of $C6_H$ and $C7_H$ suggests that degradation is balanced by microbial and seagrass derived DOM contributions along the salinity gradient. However, no significant increase in the protein-like component $C7_B$ was observed in the lake where seagrasses are abundant.

Interestingly, fluorescence intensity of peak A type component $C5_B$ in the low salinity region was nearly 0 (salinity = 0–0.5) and slightly increased with salinity. Components of similar characteristics have been reported to be produced during photodegradation of terrestrial DOM (Cawley et al., 2012a; Chen et al., 2010; Stedmon et al., 2007), and were also found in higher abundance in a canal flowing through an agricultural zone (Yamashita et al., 2010). As such, this component is most likely produced through intensive oxidative photodegradation of terrestrial DOM, particularly in Lake Akkeshi where light exposure is high, and is transported up-river through lake water intrusions. One-quarter of the Bekanbeushi River watershed is used for agricultural purposes (Woli et al., 2004), and some contributions of DOM from such activities cannot be discarded. However, since $C5_B$ was not contained in the freshwater Bekanbeushi River water, DOM in Bekanbeushi River might be mostly derived from recently photosynthesized wetland vegetation in the Bekanbeushi Marsh, which has not undergone intensive oxidative degradation (Evans et al., 2007; Raymond et al., 2007).

5.4. Harney River case study

The behavior of DOC and A_{254} along the salinity gradient was decoupled for the Harney River, where the DOC decreased while the A_{254} increased throughout the low salinity region for the Harney River (Fig. 2). An increase in A_{254} was attributed to the loadings of highly colored DOM (compared to freshwater end-member; Jaffé et al., 2004) from coastal mangrove ecosystems through tidal pumping (Cawley et al., 2013). The overall decrease in DOC is a result of predominant dilution of DOM transported towards the coast from the freshwater Everglades with higher salinity water containing lower DOC (Cawley et al., 2013; Chen et al., 2013).

While in general the fluorescence of terrestrial humic-like components tended to decrease with the increase in salinity, the intensities were above the conservative mixing line for the ubiquitous humic-like and humic acid-type components ($C1_H$, $C5_H$, $C6_H$; Fig. 5). Since similar phenomena were not observed for the Judan and Bekanbeushi Rivers, the inundation of fringe mangrove marshes and associated tidal pumping may be an important process controlling the input of CDOM along the oligo/mesohaline zone in the Harney River. Note that the amount of DOC and CDOM derived from mangroves during the dry season (March) along the Harney River was estimated to be 13 and 22% respectively (Cawley et al., 2013).

In contrast to the humic-like components, microbial humic-like component $C4_H$ and the protein-like components $C7_H$ and $C8_H$ were distributed conservatively, suggesting that these components are minor constituents of CDOM derived from mangrove ecosystems. Possible explanations for this observation is that nitrogen-containing compounds or proteinaceous materials in DOM from mangroves could have been sequestered in mangrove sediments in the form of insoluble protein–tannin complexes (Maie et al., 2008) or that phosphorus limitations in the upper estuary reduce the microbial activity (Cawley et al., 2013). Interestingly, the peak A type component $C2_H$ was conservatively distributed along the oligo/meso-haline zone, and consequently not exported from the mangrove fringe as previously suggested for the Harney and Shark river estuaries (Cawley et al., 2013). This trend might suggest that a major portion of DOM exported from periodically inundated mangrove marsh is derived from recently photosynthesized mangrove residue, and has not undergone extensive oxidative degradation like for Bekanbeushi River DOM (Evans et al., 2007; Raymond et al., 2007).

5.5. Judan River case study

In contrast to the Bekanbeushi and Harney rivers, the DOC and A_{254} distributed conservatively along the salinity gradient for the Judan River (Fig. 2). It is well known that DOC and A_{254} of open ocean water are significantly lower compared to those of terrestrial systems (Hansell et al., 2009; Nelson and Siegel, 2002; Yamashita and Tanoue, 2009). Assuming that the salinity of the open ocean water is 35 and the mixing rate of freshwater and saline water at a salinity of 5.2 is 85:15, terrestrial components would be diluted to 85% through conservative mixing. The DOC and A_{254} roughly followed this dilution rate, indicating that conservative mixing of quite high levels of terrestrial DOM and low levels of seawater DOM is the dominant process controlling the DOM dynamics in the Judan River. The river system is characterized by elevated DOC from swamp forests in peaty environments as its freshwater end-member. However, the Judan River estuary has a clear boundary between the river channel and the riverbank and is neither, associated with tidally inundated coastal wetlands like the mangrove fringe of Harney River, nor does it feature estuarine lagoons with dense seagrass communities like the Bekanbeushi River. Thus the input of DOM into the river from sources other than peat soils is considered to be small.

Notwithstanding that, DOM in the Judan River does not solely experience passive dilution, but active processing was found to occur during the mixing process. First, the fluorescence intensity of the humic acid-type component $C4_J$ decreased sharply at a very low (<1) salinity range, while such a trend was not observed for a similar component $C4_B$ in the Bekanbeushi River (Figs. 4 and 6). In addition, while the peak C type components (Table 1) generally decreased with the increase in salinity for the three coastal rivers, the fluorescence intensities of $C2_J$, $C3_J$, and $C6_J$ increased with salinity (Fig. 6), indicating the presence of a different mechanism controlling their behavior other than the dilution with seawater.

Component $C4_J$ is a fluorophore that is contained in soil humic acids in a high proportion (Ohno and Bro, 2006; Santín et al., 2009). Since humic acids intrinsically form molecular associations under acidic conditions, which can be accelerated in the presence of multi-valent cations (Baalousha et al., 2006), the low water pH in the Judan River could favor the aggregation of $C4_J$, thus removing it through flocculation and subsequent sedimentation at a low salinity range. The unique trend for $C2_J$, $C3_J$, and $C6_J$ along the salinity gradient may be attributed to the change in salinity and/or pH of river water with increasing mixing ratio of oceanic water. In previous studies, Peak C type fluorescence, where $C2_J$ and $C6_J$ are categorized (see Table 1), often increased with the increase of pH (Patel-Sorrentino et al., 2002; Spencer et al., 2007) as well as with the increase of salinity to the mesohaline zone (Boyd et al., 2010). In the research by Boyd et al. (2010), response of PARAFAC components to the salinity were different between the fast flushing period and the slow flushing period, which would indicate the existence of additional hydrological factors influence to the variations. For the Judan River, the pH of the river water increased from 3.9 at salinity 0 to 6.2 at the river mouth (salinity 5.2), which probably affected the dissociation state of acidic functional groups in DOM and/or their fluorescent quantum yield. Note that the increase of peak C type fluorescence was not observed for Bekanbeushi River where the pH did not change significantly during mixing processes in the oligohaline zone.

To investigate the influence of pH/salinity to the intensities of PARAFAC components, we conducted a model experiment in which the pH of tropical peat groundwater from the Judan River area was increased by mixing with artificial sea water (Instant Ocean®). In support of our hypothesis, the intensities of four PARAFAC components, $C2_J$, $C3_J$, $C4_J$, and $C6_J$, increased significantly with increases in pH. However, the behavior of $C4_J$ was inconsistent with this observation, as it decreased sharply along salinity gradient of the Judan River (Fig. 6). It seems that flocculation or adsorption to suspended solids and/or sediments might be playing a role in the removal of $C4_J$ in the Judan River after increased ionic strength, and thus its environmental dynamics seem unrelated to pH changes. However, the overall contribution of $C4_J$ to DOM dynamics seems small since the DOC and A_{254} behaved conservatively along salinity gradient (Fig. 2c). In addition, the changes of PARAFAC component distributions in the Judan River may have been underestimated, because EEMs were measured after diluting the original samples by a factor of 5 with Milli-Q water. This sample treatment may have resulted in a decrease in salinity and an increase in pH. Our observations, however, imply that changes in the salinity and pH throughout the entire mixing processes may lead to significant conformational changes of DOM (Blough and Zepp, 1995), which might have a significant influence on its reactivity (Osburn et al., 2009).

6. Conclusions

The results presented in this study suggest that wetland-influenced coastal rivers can have highly varied DOC concentration and DOM composition in the low salinity zone. The dynamics of DOM were found to be highly variable between wetland-associated rivers, reflecting difference in hydrology and geomorphology. For two of the three examples (Bekanbeushi and Harney rivers), a clear decoupling between DOC and CDOM was observed, while these parameters showed a conservative behavior for the third (Judan River). The DOC–CDOM decoupling was found to be driven by different mechanisms, such as inputs of non/less-colored DOM from an estuarine lake for the Bekanbeushi River, and inputs of highly colored DOM from fringe mangrove swamps along the upper estuary for the Harney River. While interplay between loss to microbial degradation and inputs from diverse sources was suggested for microbial humic-like components and protein-like components, the photo-products formed by the degradation of terrestrial-derived humic-like materials in the estuary were found to transport upstream to low salinity zones though saltwater intrusions. Lastly, possible effects on DOM dynamics as a result of change in the pH/salinity during mixing process were observed for the Judan River system draining acidic peat soils from forest swamps, suggesting changes in the dissociation state of acid functional humic-like groups and/or fluorescence quantum yield. Based on the above, it is clear that the upper river estuary, low salinity zones of wetland-influenced coastal rivers are highly dynamic

with regard to their biogeochemical trends for DOM. The application of EEM-PARAFAC demonstrated non-conservative behavior for some DOM components, and possible change of dissociation state of acidic functional group of DOM, which would not have been possible to detect using more traditional optical properties measurements.

Acknowledgments

This work was partially supported by a Grant-in-Aid for Scientific Research (B) (KAKENHI-19405021) and by a research grant from the School of Veterinary Medicine, Kitasato University (No. 2958). The Florida samples were collected as a part of a collaborative effort with the NSF-funded Florida Coastal Everglades long term ecological research program (DBI-0220409). The authors thank Mr. T. Shibutani from the Akkeshi Waterfowl Observation Center for his assistance in water sampling, and Mr. M. Tokiwa and Mr. A. Syoda from the School of Veterinary Medicine and Animal Sciences, Kitasato University, for their assistance with sample preparation and analyses. RJ thanks FIU for additional support through the George Barley Chair during this study. This is SERC contribution #663.

References

Abe, Y., Maie, N., Shima, E., 2011. Influence of irrigated paddy fields on the fluorescence properties of fluvial dissolved organic matter. J. Environ. Qual. 40, 1266–1272.
Asmala, E., Stedmon, C.A., Thomas, D.N., 2012. Linking CDOM spectral absorption to dissolved organic carbon concentrations and loadings in boreal estuaries. Estuar. Coast. Shelf Sci. 111, 107–117.
Baalousha, M., Motelica-Heino, M., Le Coustumer, P., 2006. Conformation and size of humic substances: Effects of major cation concentration and type, pH, salinity, and residence time. Colloids Surf., A 272, 48–55.
Barrón, C., Apostolaki, E.T., Duarte, C.M., 2012. Dissolved organic carbon release by marine macrophytes. Biogeosci. Discuss. 9, 1529–1555.
Bertilsson, S., Jones Jr., J.B., 2003. Supply of dissolved organic matter to aquatic ecosystems: autochthonous sources. In: Findlay, S.E.G., Sinsabaugh, R.L. (Eds.), Aquatic Ecosystems: Interactivity of Dissolved Organic Matter. Academic Press, San Diego, pp. 2–24.
Blough, N.V., Zepp, R.G., 1995. Reactive oxygen species in natural waters. In: Foote, C.S., Valentine, J.S., Greenberg, A., Liebman, J.F. (Eds.), Active Oxygen: Reactive Oxygen Species in Chemistry. Blackie Academic & Professional, London, pp. 280–333.
Boyd, T.J., Barham, B.P., Hall, G.J., Osburn, C.L., 2010. Variation in ultrafiltered and LMW organic matter fluorescence properties under simulated estuarine mixing transects: 1. Mixing alone. J. Geophys. Res. 115, G00F13. http://dx.doi.org/10.1029/2009JG000992.
Cauwet, G., 2002. DOM in the coastal zone. In: Hansell, D.A., Carlson, C.A. (Eds.), Biogeochemistry of Marine Dissolved Organic Matter. Academic Press, San Diego, pp. 579–609.
Cawley, K., Wolski, P., Mladenov, N., Jaffé, R., 2012a. Dissolved organic matter biogeochemistry along a transect of the Okavango Delta, Botswana. Wetlands. http://dx.doi.org/10.1007/s13157-012-0281-0.
Cawley, K., Ding, Y., Fourqurean, J.W., Jaffé, R., 2012b. Characterizing the sources and fate of dissolved organic matter in Shark Bay, Australia: a preliminary study using optical properties and stable carbon isotopes. Mar. Freshw. Res. 63, 1098–1107.
Cawley, K., Yamashita, Y., Maie, N., Jaffé, R., 2013. Using optical properties to quantify fringe mangrove inputs to the dissolved organic matter (DOM) pool in a subtropical estuary. Estuar. Coasts. http://dx.doi.org/10.1007/s12237-013-9681-5.
Chen, M., Price, R.M., Yamashita, Y., Jaffé, R., 2010. Comparative study of dissolved organic matter from groundwater and surface water in the Florida coastal Everglades using multi-dimensional spectrofluorometry combined with multivariate statistics. Appl. Geochem. 25, 872–880.
Chen, M., Maie, N., Parish, K., Jaffé, R., 2013. Spatial and temporal variability of dissolved organic matter quantity and composition in an oligotrophic subtropical coastal wetland. Biogeochemistry. http://dx.doi.org/10.1007/s10533-013-9826-4.
Chin, Y.-P., Aiken, G., O'Loughlin, E., 1994. Molecular weight, polydispersity, and spectroscopic properties of aquatic humic substances. Environ. Sci. Technol. 28, 1853–1858.
Cifuentes, L.A., Eldridge, P.M., 1998. A mass- and isotope-balance model of DOC mixing in estuaries. Limnol. Oceanogr. 43, 1872–1882.
Coble, P.G., 2007. Marine optical biogeochemistry: The chemistry of ocean color. Chem. Rev. 107 (2), 402–418. http://dx.doi.org/10.1021/cr050350.
Coble, P.G., Del Castillo, C.E., Bernard, A., 1998. Distribution and optical properties of CDOM in the Arabian Sea during the 1995 Southwest Monsoon. Deep-Sea Res. II 45, 2195–2223.
Cory, R., Mcknight, D.M., 2005. Fluorescence spectroscopy reveals ubiquitous presence of oxidized and reduced quinones in dissolved organic matter. Environ. Sci. Technol. 39, 8142–8149.
Dalzell, B.J., Minor, E.C., Mopper, K.M., 2009. Photodegradation of estuarine dissolved organic matter: a multi-method assessment of DOM transformation. Org. Geochem. 40, 243–257.
Davis, S.M., Ogden, J.C. (Eds.), 1994. Everglades: The Ecosystem and its Restoration. St. Lucie Press, Boca Raton.
Dittmar, T., Hertkorn, N., Kattner, G., Lara, R.J., 2006. Mangroves, a major source of dissolved organic carbon to the oceans. Global Biogeochem. Cycles 20, GB1012. http://dx.doi.org/10.1029/2005GB002570.
Dittmar, T., Paeng, J., Gihring, T.M., Suryaputra, I.G.N.A., Huettel, M., 2012. Discharge of dissolved black carbon from a fire-affected intertidal system. Limnol. Oceanogr. 57, 1171–1181. http://dx.doi.org/10.4319/lo.2012.57.4.1171.
Evans, C.D., Freeman, C., Cork, L.G., Thomas, D.N., Raynolds, B., Billett, M.F., Garnett, M.H., Norris, D., 2007. Evidence against recent climate-induced destabilisation of soil carbon from C-14 analysis of riverine dissolved organic matter. Geophys. Res. Lett. 34, L07407. http://dx.doi.org/10.1029/2007GL029431.
Fellman, J.B., Hood, E., D'Amore, D.V., Edwards, R.T., White, D., 2009. Seasonal changes in the chemical quality and biodegradability of dissolved organic matter exported from soils to streams in coastal temperate rainforest watersheds. Biogeochemistry 95, 277–293.
Fellman, J.B., Spencer, R.G.M., Hernes, P.J., Edwards, R.T., D'Amore, D.V., Hood, E., 2010a. The impact of glacier runoff on the biodegradability and biochemical composition of terrigenous dissolved organic matter in near-shore marine ecosystems. Mar. Chem. 121, 112–122.
Fellman, J.B., Hood, E., Spencer, R.G.M., 2010b. Fluorescence spectroscopy opens new window into dissolved organic matter dynamics in freshwater ecosystems: a review. Limnol. Oceanogr. 55, 2452–2462.
Fellman, J.B., Petrone, K.C., Grierson, P.F., 2011. Source, biogeochemical cycling, and fluorescence characteristics of dissolved organic matter in an agro-urban estuary. Limnol. Oceanogr. 56, 243–256.
Fichot, C.G., Benner, R., 2011. A novel method to estimate DOC concentrations from CDOM absorption coefficients in coastal waters. Geophys. Res. Lett. 38, L03610. http://dx.doi.org/10.1029/2010GL046152.
Hansell, D.A., Carlson, C.A., Repeta, D.J., Schlitzer, R., 2009. Dissolved organic matter in the ocean: a controversy stimulates new insights. Oceanography 22 (4), 202–211.
Hasegawa, N., Hori, M., Mukai, H., 2007. Seasonal shifts in seagrass bed primary producers in a cold-temperate estuary: Dynamics of eelgrass *Zostera marina* and associated epiphytic algae. Aquat. Bot. 86 (4), 337–345.
Hedges, J.I., 1992. Global biogeochemical cycles-progress and problems. Mar. Chem. 39, 67–93.
Hedges, J.I., Keil, R.G., Benner, R., 1997. What happens to terrestrial organic matter in the ocean? Org. Geochem. 27, 195–212.
Ishii, S.K.L., Boyer, T.H., 2012. Behavior of reoccurring PARAFAC components in fluorescent dissolved organic matter in natural and engineered systems: a critical review. Environ. Sci. Technol. 46, 2006–2017. http://dx.doi.org/10.1021/es2043504.
Jaffé, R., Boyer, J.N., Lu, X., Maie, N., Yang, C.-Y., Scully, N.M., Mock, S., 2004. Source characterization of dissolved organic matter in a subtropical mangrove-dominated estuary by fluorescence analysis. Mar. Chem. 84, 195–210.
Jaffé, R., McKnight, D., Maie, N., Cory, R., McDowell, W.H., Campbell, J.L., 2008. Spatial and temporal variations in DOM composition in ecosystems: the importance of long-term monitoring of optical properties. J. Geophys. Res. 113, G04032. http://dx.doi.org/10.1029/2008JG000683.
Japan Metrological Agency, 2010. Retrieved from Meteorological database. http://www.data.jma.go.jp/gmd/risk/obsdl/index.php.
Lapierre, J.-F., Frenette, J.J., 2009. Effects of macrophytes and terrestrial inputs on fluorescent dissolved organic matter in a large river system. Aquat. Sci. 71, 15–24.
Maie, N., Yang, C.-Y., Miyoshi, T., Parish, K., Jaffé, R., 2005. Chemical characteristics of dissolved organic matter in an oligotrophic subtropical wetland/estuarine ecosystem. Limnol. Oceanogr. 50 (1), 23–35.
Maie, N., Miyoshi, T., Childers, D.L., Jaffé, R., 2006. Quantitative and qualitative aspects of dissolved organic carbon leached from plants in an oligotrophic wetland. Biogeochemistry 78, 285–314.
Maie, N., Pisani, O., Jaffé, R., 2008. Mangrove tannins in aquatic ecosystems: their fate and possible influence on dissolved organic carbon and nitrogen cycling. Limnol. Oceanogr. 53, 160–171.
Maie, N., Yamashita, Y., Cory, R., Boyer, J., Jaffé, R., 2012. Application of excitation emission matrix fluorescence monitoring in the assessment of spatial and seasonal drivers of dissolved organic matter composition: sources and physical disturbance controls. Appl. Geochem. 27, 917–929. http://dx.doi.org/10.1016/j.apgeochem.2011.12.021.
McKnight, D.M., Boyer, E.W., Westerhoff, P.K., Doran, P.T., Kulbe, T., Andersen, D.T., 2001. Spectrofluorometric characterization of dissolved organic matter for indication of precursor organic material and aromaticity. Limnol. Oceanogr. 46, 38–48.
Mitsch, W.J., Gosselink, J.G., 2007. Wetlands, 4th ed. John Wiley & Sons, New York (582 pp.).
Moore, S., Gauci, V., Evans, C.D., Page, S.E., 2011. Fluvial organic carbon losses from a Bornean blackwater river. Biogeosciences 8, 901–909.
Mulholland, P.J., 2003. Large-scale patterns in dissolved organic carbon concentration, flux, and sources. In: Findlay, S.E.G., Sinsabaugh, R.L. (Eds.), Aquatic Ecosystems: Interactivity of Dissolved Organic Matter. Academic Press, San Diego, pp. 139–159.
Nelson, N.B., Siegel, D.A., 2002. Chromophoric DOM in the open ocean. In: Hansell, D.A., Carlson, C.A. (Eds.), Biogeochemistry of Marine Dissolved Organic Matter. Academic Press, San Diego, pp. 547–578.
Ohno, T., Bro, R., 2006. Dissolved organic matter characterization using multiway spectral decomposition of fluorescence landscapes. Soil Sci. Soc. Am. J. 70, 2028–2037. http://dx.doi.org/10.2136/sssaj2006.0005.
Osburn, C.L., Stedmon, C.A., 2011. Linking the chemical and optical properties of dissolved organic matter in the Baltic-North Sea transition zone to differentiate three allochthonous inputs. Mar. Chem. 126 (1–4), 281–294.
Osburn, C.L., O'Sullivan, D.W., Boyd, T.J., 2009. Increase in the longwave photobleaching of chromophoric dissolved organic matter in coastal waters. Limnol. Oceanogr. 54, 145–159.
Patel-Sorrentino, N., Mounier, S., Benaim, J.Y., 2002. Excitation-emission fluorescence matrix to study pH influence on organic matter fluorescence in the Amazon basin rivers. Water Res. 36, 2571–2581.

Raymond, P.A., McClelland, J.W., Holmes, R.M., Zhulidov, A.V., Mull, K., Peterson, B.J., Striegl, R.G., Aiken, G.R., Gurtovaya, T.Y., 2007. Flux and age of dissolved organic carbon exported to the Arctic Ocean: a carbon isotopic study of the five largest Arctic rivers. Glob. Biogeochem. Cycles 21, GB4011. http://dx.doi.org/10.1029/2007GB002934.

Santín, C., Yamashita, Y., Otero, X.L., Álvarez, M.Á., Jaffé, R., 2009. Characterizing humic substances from estuarine soils and sediments by excitation–emission matrix spectroscopy and parallel factor analysis. Biogeochemistry 96, 131–147.

Singh, S., D'Sa, E.J., Swenson, E.M., 2010. Chromophoric dissolved organic matter (CDOM) variability in Barataria Basin using excitation–emission matrix (EEM) fluorescence and parallel factor analysis (PARAFAC). Sci. Total Environ. 408, 3211–3222.

Spencer, R.G.M., Bolton, L., Baker, A., 2007. Freeze/thaw and pH effects on freshwater dissolved organic matter fluorescence and absorbance properties from a number of UK locations. Water Res. 41, 2941–2950.

Stedmon, C.A., Bro, R., 2008. Characterizing dissolved organic matter fluorescence with parallel factor analysis: a tutorial. Limnol. Oceanogr. Methods 6, 572–579.

Stedmon, C.A., Markager, S., 2005. Tracing the production and degradation of autochthonous fractions of dissolved organic matter by fluorescence analysis. Limnol. Oceanogr. 50 (5), 1415–1426.

Stedmon, C.A., Markager, S., Bro, R., 2003. Tracing dissolved organic matter in aquatic environments using a new approach to fluorescence spectroscopy. Mar. Chem. 82, 239–254.

Stedmon, C.A., Markager, S., Tranvik, L., Kronberg, L., Slatis, T., Martinsen, W., 2007. Photochemical production of ammonium and transformation of dissolved organic matter in the Baltic Sea. Mar. Chem. 104, 227–240.

Tzortziou, M., Neale, P.J., Osburn, C.L., Megonigal, J.P., Maie, N., Jaffé, R., 2008. Tidal marshes as a source of optically and chemically distinctive colored dissolved organic matter in the Chesapeake Bay. Limnol. Oceanogr. 53, 148–159.

Watanabe, A., Moroi, K., Sato, H., Tsutsuki, K., Maie, N., Melling, L., Jaffe, R., 2012. Contributions of humic substances to the dissolved organic carbon pool in wetlands from different climates. Chemosphere 88, 1265–1268.

Weishaar, J.L., Aiken, G.R., Bergamaschi, B.A., Fram, M.S., Fujii, R., Mopper, K., 2003. Evaluation of specific ultraviolet absorbance as an indicator of the chemical composition and reactivity of dissolved organic carbon. Environ. Sci. Technol. 37, 4702–4708.

Williams, C.J., Yamashita, Y., Wilson, H.F., Jaffé, R., Xenopoulos, M.A., 2010. Unraveling the role of land use and microbial activity in shaping dissolved organic matter characteristics in stream ecosystems. Limnol. Oceanogr. 55 (3), 1159–1171. http://dx.doi.org/10.4319/lo.2010.55.3.1159.

Woli, K.P., Nagumo, T., Kuramochi, K., Hatano, R., 2004. Evaluating river water quality through land use analysis and N budget approaches in livestock farming areas. Sci. Total Environ. 329, 61–74.

Yamashita, Y., Tanoue, E., 2003. Chemical characterization of protein-like fluorophores in DOM in relation to aromatic amino acids. Mar. Chem. 82, 255–271.

Yamashita, Y., Tanoue, E., 2009. Basin scale distribution of chromophoric dissolved organic matter in the Pacific Ocean. Limnol. Oceanogr. 54, 598–609.

Yamashita, Y., Jaffé, R., Maie, N., Tanoue, E., 2008. Assessing the dynamics of dissolved organic matter (DOM) in coastal environments by excitation emission matrix fluorescence and parallel factor analysis (EEM-PARAFAC). Limnol. Oceanogr. 53, 1900–1908.

Yamashita, Y., Scinto, L.J., Maie, N., Jaffé, R., 2010. Dissolved organic matter characteristics across a subtropical wetland's landscape: application of optical properties in the assessment of environmental dynamics. Ecosystems. http://dx.doi.org/10.1007/s10021-010-9370-1.

Ziegler, J.C., Benner, R., 1999. Dissolved organic carbon cycling in a subtropical seagrass-dominated lagoon. Mar. Ecol. Prog. Ser. 180, 149–160.